Long-term Variability in the Length of the Solar Cycle

Michael L. Rogers, Mercedes T. Richards

Department of Astronomy & Astrophysics, Penn State University, 525 Davey Laboratory, University Park, PA, 16802-6305

mrogers@astro.psu.edu, mrichards@astro.psu.edu

and

Donald St. P. Richards

Department of Statistics, Penn State University, 326 Thomas Building, University Park, PA, 16802-2111

richards@stat.psu.edu

ABSTRACT

We have analyzed archival data of sunspot numbers from 1700 - 2005 and sunspot areas from 1874 - 2005 to derive the solar activity cycles based on these variables. This re-examination was motivated by the unexpectedly high level of solar activity during Solar Cycle 23 which occurred three years after the predicted cycle maximum. Two independent techniques were used in this analysis, namely power spectrum analysis and phase dispersion minimization. Our analyses confirmed the $\sim$11-year Schwabe Cycle and the $\sim$22-year Hale Cycle, and illustrated that the Schwabe Cycle is actually the average of a varying cycle which typically ranges from $\sim$10 – 12 years. Archival data from 1610 - 1990 were used to identify long-term cycles from median trace analyses of the length of the sunspot cycle, and also from power spectrum analyses of the (O-C) residuals of the dates of sunspot minima and maxima. The median trace analysis suggests that the length of the sunspot cycle varies with a period of 183 - 243 years, while the power spectrum analysis identified a secular period of 188 $\pm$ 38 years. We found a correlation between the times of historic minima and the length of the sunspot cycle. In particular, the length of the sunspot cycle was usually highest when the actual number of sunspots was lowest.

Subject headings: stars: activity – stars: flare – stars: individual (Sun) – Sun: sunspots

1. Introduction

Solar Cycle 23 was predicted to reach a maximum in early 2000 (Joselyn et al. 1996), with severe geomagnetic storms expected between 1999 and 2005. Nevertheless, the high level of solar activity exhibited through flares in 2003 October and November, including some of the most powerful solar flares ever detected, was still unexpected because this activity occurred three years after the predicted maximum of the solar cycle. In light of this unanticipated activity, it is natural to un-

dertake a deeper investigation of the solar activity cycle. In this work, we have reanalyzed archival data of sunspot numbers and areas to examine the variability in the length of the solar cycle. A summary of earlier analyses of the sunspot cycle is given by Kuklin (1976).

For more than two centuries, solar physicists have applied a variety of techniques to determine the nature of the solar cycle. The earliest methods involved counting sunspot numbers and determining durations of cyclic activity from sunspot minimum to minimum, as well as sunspot maxi-

mum to maximum (Wilson 1994). More recently, since 1874, sunspot areas have been recorded to give a total surface area of the solar disk covered by sunspots at a given time (Hathaway 2004). These types of approaches are often dubbed a one-dimensional approach because there is only one independent variable involved, namely sunspot numbers or sunspot areas (Wilson 1994).

There is also a two-dimensional approach in which the latitude of an observed sunspot is introduced as a second independent variable (Wilson 1994). When sunspots first appear on the solar surface they tend to originate in latitudes around 40 degrees and migrate toward the solar equator. When such migrant activity is taken into account it can be shown that there is an overlap between successive cycles, since a new cycle begins while its predecessor is still decaying. This overlap became obvious when Maunder, in 1922, published his butterfly diagram and demonstrated the latitude drift of sunspots throughout the cycles (Wilson 1994). Maunder's butterfly diagram showed that although the length of time between sunspot minima is on average 11 years, successive cycles actually overlap by $\sim$ 1 to 2 years.

Sunspot number data collected prior to the 1700's show epochs in which there were almost no sunspots visible on the solar surface. One such epoch, known as the Maunder Minimum, occurred between the years 1642 and 1705, during which the number of sunspots recorded were very low in comparison to later epochs (Wilson 1994). Other studies include the analysis of geophysical data and tree-ring radiocarbon data, which contain residual traces of solar activity (Baliunas & Vaughan 1985), to determine if the Maunder period truly had a lower number of sunspots or whether it was simply a period in which little data were collected or large degrees of errors existed. While the data collected before the 1700's are typically less reliable than those collected in more recent times, the timing of the Maunder Minimum is still relatively accurate because of the correlation with geophysical data. Other epochs of minimum solar activity in the past have been noted, such as: the Dalton Minimum from 1795 - 1823 (Soon & Yaskell 2003), the Spörer Minimum from 1420 - 1530, the Wolf Minimum from 1280 - 1340, and the Oort Minimum from 1010 - 1050 (Eddy 1977; Stuiver & Quay 1980; Siscoe 1980). These minima

have been derived from historical sunspot records, auroral histories (Eddy 1976), and physical models linking dendrochronologically dated radiocarbon concentrations to the solar cycle (Solanki et al. 2004).

In this paper, we have applied classical one-dimensional techniques to rederive the periodicities of solar activity using sunspot number and area data. These results were used as a basis in the examination of the secular behavior of the length of the sunspot number cycle.

2. Data Collection

The sunspot data were collected from archival sources that catalog sunspot numbers, sunspot areas, as well as the measured length of the sunspot cycle. The sunspot number data, ranging from 1700 - 2005, are archived by the National Geophysical Data Center (NGDC). These data are listed in individual sets of daily, monthly, and yearly numbers. The relative sunspot number, R, is defined as R = K (10g + s), where g is the number of sunspot groups, s is the total number of distinct spots, and the scale factor K (usually less than unity) depends on the observer and is "intended to effect the conversion to the scale originated by Wolf" (Coffey & Erwin 2004). The scale factor was 1 for the original Wolf sunspot number calculation. The spot number data sets are tabulated in Table 1 and plotted in Figure 1.

The sunspot area data, beginning in 1874 May 9, were compiled by the Royal Greenwich Observatory from a small network of observatories (Hathaway 2004). In 1976, the United States Air Force began compiling its own database from its Solar Optical Observing Network (SOON). The work continued with the help of the National Oceanic and Atmospheric Administration (NOAA) (Hathaway 2004). The NASA compilation of these separate data sets lists sunspot area as the total whole spot area in millionths of solar hemispheres. We have analyzed the compiled daily sunspot areas as well as their monthly and yearly sums. The sunspot area data sets are tabulated in Table 1 and plotted in Figure 2.

The sunspot number cycle data were tabulated by the NGDC (Coffey & Erwin 2004) and are discussed further in §4. These data span dates from 1610 to 1990 (Table 2).

TABLE 1

DURATION OF THE DATA

Data Set		Duration of Data
Spot Numbers	Daily	1818 Jan 8 - 2005 Jan 31
	Monthly	1749 Jan - 2005 Jan
	Yearly	1700 - 2004
Spot Areas	Daily	1874 May 9 - 2005 Feb 28
	Monthly	1874 May - 2005 Feb
	Yearly	1874 - 2004

3. Sunspot Numbers and Areas

The sunspot number and sunspot area data were analyzed with the same techniques that were used by Richards, Waltman, Ghigo, & Richards (2003) in their study of radio flaring cycles of magnetically active close binary star systems.

3.1. Power Spectrum & PDM Analyses

Two independent methods were used to determine the solar activity cycles. In the first method, we analyzed the power spectrum obtained by calculating the Fast Fourier transform (FFT) of the data. The Fourier transform of a function $h(t)$ is described by $H(\nu) = \int h(t) \, e^{2\pi i \nu t} dt$ for frequency, ν, and time, t. This transform becomes a δ function at frequencies that correspond to true periodicities in the data, and subsequently the power spectrum will have a sharp peak at those frequencies. The Lomb-Scargle periodogram analysis for unevenly spaced data was used (Press et al. 1992).

In the second method, called the Phase Dispersion Minimization (PDM) technique (Stellingwerf 1978), a test period was chosen and checked to determine if it corresponded to a true periodicity in the data. The goodness of fit parameter, Θ, approaches zero when the test period is close to a true periodicity. PDM produces better results than the FFT in the case of non-sinusoidal data. The goodness of fit between a test period Π and a true period, P_{true} is given by the statistic, $\Theta = s^2/\sigma_t^2$ where, the data are divided into M groups or samples,

$$\sigma_t^2 = \frac{\sum(x_i - \bar{x})^2}{(N-1)}, \qquad s^2 = \frac{\sum(n_j - 1)s_j^2}{(\sum n_j - M)},$$

s^2 is the variance of M samples within the data set, x_i is a data element (S_ν), $\bar{x}$ is the mean of the data, N is the number of total data points, n_j is number of data points contained in the sample M, and s_j is the variance of the sample M. If $\Pi \neq P_{true}$, then $s^2 = \sigma_t^2$ and $\Theta = 1$. However, if $\Pi = P_{true}$, then $\Theta \to 0$ (or a local minimum).

All solutions from the two techniques were checked for numerical relationships with (i) the highest frequency of the data (corresponding to the data sampling interval), (ii) the lowest frequency of the data, dt (corresponding to the duration or time interval spanned by the data), (iii) the Nyquist frequency, $N/(2dt)$, and in the case of PDM solutions (iv) the maximum test period assumed. A maximum test period of 260 years was chosen for all data sets, except in the case of the more extensive yearly sunspot number data when a maximum of 350 years was assumed. We chose the same maximum test period for the sunspot area analysis for consistency with the sunspot number analysis, even though these test periods are longer than the duration of the area data.

3.2. Results of Power Spectrum and PDM Analyses

The results from the FFT and PDM analyses of sunspot number and sunspot area data are illustrated in Figures 3 & 4, corresponding to the daily, monthly, and yearly sunspot numbers and the daily, monthly, and yearly sunspot areas, respectively. In these figures, the top frame shows the power spectrum derived from the FFT analysis, while the bottom frame shows the Θ-statistic obtained from the PDM analysis.

The sunspot cycles derived from these results

TABLE 2

LENGTH OF THE SUNSPOT CYCLE

Year of Minimum	Year of Maximum	Cycle Length (yr) (from minima)	Cycle Length (yr) (from maxima)
1610.8	1615.5	8.2	10.5
1619.0	1626.0	15.0	13.5
1634.0	1639.5	11.0	9.5
1645.0	1649.0	10.0	11.0
1655.0	1660.0	11.0	15.0
1666.0	1675.0	13.5	10.0
1679.5	1685.0	9.5	8.0
1689.0	1693.0	9.0	12.5
1698.0	1705.5	14.0	12.7
1712.0	1718.2	11.5	9.3
1723.5	1727.5	10.5	11.2
1734.0	1738.7	11.0	11.6
1745.0	1750.3	10.2	11.2
1755.2	1761.5	11.3	8.2
1766.5	1769.7	9.0	8.7
1775.5	1778.4	9.2	9.7
1784.7	1788.1	13.6	17.1
1798.3	1805.2	12.3	11.2
1810.6	1816.4	12.7	13.5
1823.3	1829.9	10.6	7.3
1833.9	1837.2	9.6	10.9
1843.5	1848.1	12.5	12.0
1856.0	1860.1	11.2	10.5
1867.2	1870.6	11.7	13.3
1878.9	1883.9	10.7	10.2
1889.6	1894.1	12.1	12.9
1901.7	1907.0	11.9	10.6
1913.6	1917.6	10.0	10.8
1923.6	1928.4	10.2	9.0
1933.8	1937.4	10.4	10.1
1944.2	1947.5	10.1	10.4
1954.3	1957.9	10.6	11.0
1964.9	1968.9	11.6	11.0
1976.5	1979.9	10.3	9.7
1986.8	1989.6	11.1	11.0
		Avg.=11.1±1.5	Avg.=11.0±2.0

4

are summarized in Table 3. The most significant periodicities corresponding to the 50 highest powers and the 50 lowest θ values suggest that the solar cycle derived from sunspot numbers is 10.95 ± 0.60 years, while the value derived from sunspot area is 10.65 ± 0.40 years. The average sunspot cycle from both the number and area data is 10.80 ± 0.50 years. The strongest peaks in Figures 3 & 4 correspond to this dominant average periodicity over a range from ~ 8 years up to ~ 12 years. A weaker periodicity was also identified from the PDM analysis with an average period of 21.90 ± 0.66 years over a range from ~ 20 - 24 years.

The errors for the FFT and PDM analyses were derived by measuring the Full Width at Half Maximum ($FWHM$) of each dominant peak for each data set. The 1σ error is then defined by $\sigma = FWHM/2.35$. The three averages given in Table 3 were determined by averaging the dominant solutions from the FFT and PDM analyses for each data set. The errors in the averages were determined using standard techniques (Bevington 1969; Topping 1972). While the errors for the sunspot area results are smaller than those for the spot numbers, the area data are actually less accurate than the sunspot number data because the measurement error in the areas may be as high as 30% (Hathaway 2004). The higher errors for the area data are related to the difficulty in determining a precise spot boundary.

Longer periodicities that could not be eliminated because of relationships with the duration of the data set or other frequencies related to the data (as described in §3.1), were also identified with durations ranging from ~ 90 - 260 years (Figures 3 & 4). These long-term periodicities are discussed further in the following section.

4. Sunspot Cycle Minima and Maxima

The previous analysis of sunspot data provided some evidence of long term cycles in the sunspot data. This secular behavior was studied in greater detail through an analysis of the dates of sunspot minima and maxima from 1610 to 1990 tabulated by the NGDC (Coffey & Erwin 2004). Sunspot cycle lengths were derived by the NGDC from the dates of successive cycle minima. In addition, we have used their tabulated dates of cycle maxima to calculate the corresponding cycle lengths. These

cycle lengths are tabulated in Table 2 and plotted in Figure 5. The data in Figure 5 show substantial variability over time.

The cycle lengths derived from the dates of sunspot minima and maxima were analyzed to search for periodicities in the cycle length using two techniques: (i) a median trace analysis and (ii) a power spectrum analysis of the 'Observed minus Calculated' or (O-C) residuals.

4.1. Median Trace Analysis

A median trace is a plot of the median value of the data contained within a bin of a chosen width, for all bins in the data set. The median trace analysis depends on the choice of an optimal interval width (OIW). These OIWs, h_n, were calculated using three statistical methods based on theoretical arguments used routinely to estimate the statistical density function of the data (Hoaglin et al. 1983). The first method defines the OIW as

$$h_{n,1} = \frac{3.49 \, \tilde{s}}{n^{1/3}} \qquad (1)$$

where n is the number of data points and $\tilde{s}$, a statistically robust measure of the standard deviation of the data, is defined as

$$\tilde{s} = \frac{1}{n} \sum_{i=1}^{n} |x_i - M| \, , \qquad (2)$$

where M is the sample median. The second method defines the OIW as

$$h_{n,2} = 1.66 \, \tilde{s} \left(\frac{\log_e n}{n} \right)^{1/3} . \qquad (3)$$

A third definition of the OIW is given by

$$h_{n,3} = \frac{2 \times IQR}{n^{1/3}} \, , \qquad (4)$$

where IQR is the interquartile range of the data set. Optimal bin widths were determined for three data sets corresponding to the cycle lengths derived from the (i) cycle minima, (ii) cycle maxima, and (iii) the combined minima and maxima data. Table 4 lists the solutions for the optimal interval widths ($h_{n,1}, h_{n,2}, h_{n,3}$) for each data set.

Since the values of the optimal bin widths ranged from ~ 60 - 120 years, we tested the impact

TABLE 3

SOLAR ACTIVITY CYCLES DERIVED FROM FFT & PDM ANALYSES

| Data Set | | Schwabe Cycle (years) | | Hale Cycle (years) |
		FFT	PDM	PDM
Sunspot Numbers	daily	10.85 ± 0.60	10.86 ± 0.27	22.08 ± 0.59
	monthly	11.01 ± 0.68	11.02 ± 0.68	21.80 ± 0.90
	yearly	10.95 ± 0.72	11.01 ± 0.64	22.32 ± 1.05
Average (Numbers)			10.95 ± 0.60	22.07 ± 0.85
Sunspot Areas	daily	10.67 ± 0.44	10.67 ± 0.42	21.77 ± 0.46
	monthly	10.67 ± 0.39	10.66 ± 0.39	21.76 ± 0.46
	yearly	10.62 ± 0.39	10.62 ± 0.36	21.68 ± 0.47
Average (Areas)			10.65 ± 0.40	21.74 ± 0.46
Combined Average			10.80 ± 0.50	21.90 ± 0.66

TABLE 4

OPTIMUM INTERVAL WIDTHS

| Data Set | No. Data | Standard Deviation | Optimum Bin Widths (years) | | |
	n	$\tilde{s}$ (years)	$h_{n,1}$	$h_{n,2}$	$h_{n,3}$
Cycle Minima	35	97.4	103.9	75.4	116.6
Cycle Maxima	35	97.0	103.4	75.1	115.4
Combined Data	70	97.3	82.4	63.5	91.8

TABLE 5

PREDICTED PERIODICITIES OF SUNSPOT NUMBER CYCLE

| Bin Width (years) | Predicted Periodicities (years) | | | |
	Minima	Maxima	Combined	Average
40	157	165	146	156 ± 10
50	185	182	182	183 ± 2
60	243	243	243	243
70	222	273	304	266 ± 41
80	393	349	419	387 ± 35
90	299	299	209	269 ± 52

of different bin widths on our results. This procedure was limited by the fact that only 35 sunspot number cycles have elapsed since 1610 (see Table 2). The data set can be increased to 70 points if we analyze the combined values of the length of the solar cycle derived from both the sunspot minima and the sunspot maxima. Using our derived OIWs as a basis for our analysis, we calculated median traces for bin widths of 40, 50, 60, 70, 80, and 90 years. These are illustrated in Figure 6. The lower bin widths were included to make maximum use of the limited number of data points, and the higher bin widths were excluded because, once binned, there would be too few data points to make those analyses meaningful.

Figure 6 shows the original data, the binned data (median values), and sinusoidal fits to the binned data. The Least Absolute Error Method (Bates & Watts 1988) was used to produce the sinusoidal fits to the median trace in each frame of the figure. These sinusoidal fits illustrate the long-term cyclic behavior in the length of the sunspot number cycle.

4.2.   Results of Median Trace Analysis

The lengths of the sunspot number cycles tabulated by the National Geophysical Data Center (Table 2 & Figure 5) show that the basic sunspot number cycle is an average of (11.1 ± 1.5) years based on the cycle minima and (11.0 ± 2.0) years based on the cycle maxima. This Schwabe Cycle varies over a range from 8 to 15 years if the cycle lengths are derived from the time between successive minima, while the range increases to 7 to 17 years if the cycle lengths are derived from successive maxima. These variations may be significant even though the data in Figure 5 show *heteroskedasticity*, i.e., variability in the standard deviation of the data over time. Although the range in sunspot cycle durations is large, the cycle length converges to a mean of 11 years, especially after 1818 when the accuracy of the data became more reliable. In particular, the sunspot number cycle lengths from 1610 - 1750 shows a wide range of variance while the cycle durations since 1818 show a much smaller variance (Figure 5). This variance may be influenced by the difficulty in identifying the dates of cycle minima and maxima whenever the sunspot activity is relatively low. Even after the data became more accurate there was still

a significant $\pm$ 1.5-year range about the 11-year mean. The range in the length of this cycle suggests that there may be a hidden longer-term variability in the Schwabe cycle.

Our median trace analysis of the lengths of the sunspot number cycle uncovered a long-term cycle with a duration between 146 and 419 years, if the data are binned in groups of 40 to 90 years (see §4.1). The predicted cycle periods are listed in Table 5 for all three data sets: the (a) cycle minima, (b) cycle maxima, and (c) combined minima and maxima data. Since the median trace analysis is influenced by the bin size of the data, we determined the optimum bin width based on the goodness of fit between the median trace and the corresponding sinusoidal fit. Figure 6 shows the median traces for the data and illustrates that the optimum bin width is in the range of 50 - 60 years (Figure 8). Moreover, it is only in these two cases that the sinusoidal fits are in phase for all three data sets. The 50-year median trace predicts a 183-year sunspot number cycle, while the 60-year trace predicts a 243-year cycle. Similar long-term cycles ranging from 169 to 189 years have been proposed for several decades (Kuklin 1976).

4.3.   Analysis of the (O-C) Data

The median trace analysis gives us a rough estimate of the long-term sunspot cycle. However, an alternative method to derive this secular period is to calculate the power spectrum of the (O-C) variation of the dates corresponding to the (i) cycle minima, (ii) cycle maxima, and (iii) the combined minima and maxima.

The following procedure was used to calculate the (O-C) residuals for each of the data sets given above, based only on the dates of minima and maxima listed in Table 2. First, we defined the cycle number, ϕ, to be $\phi = (t_i - t_0)/L$, where t_i are the individual dates of the extrema, and t_0 is the start date for each data set. Here, L is the average cycle length (10.95 years) derived independently by the FFT and PDM analyses from the sunspot number data (§3.2). The (O-C) residuals were defined to be

$$(O - C) = (t_i - t_0) - (N_c \times L)$$

where, N_c is the integer part of ϕ and represents the whole number of cycles that have elapsed since

the start date. The resulting (O-C) pattern was normalized by subtracting the linear trend in the data. This trend was found by fitting a least squares line to the (O-C) data. The normalized (O-C) data are shown in Figure 7 along with the corresponding power spectra.

4.4. Results of (O-C) Data Analysis

The power spectra of the (O-C) data in Figure 7 show that the long term variation in the sunspot number cycle has a dominant period of 188 ± 38 years. The Gleissberg cycle was also identified in this analysis, with a period of 87 ± 13 years. The solutions for these analyses are illustrated in Figure 7 and tabulated in Table 6. The 1σ errors were calculated from the FWHM of the power spectrum peaks, as described in Section 3.2. The sinusoidal fit to the (O-C) data in Figure 7 corresponds to the dominant periodicity of 188 years identified in the power spectra. Another cycle with a period of ~ 40 years was also found.

5. Discussion and Conclusions

The results of the FFT and PDM analyses of sunspot number and area data have shown that the Schwabe Cycle has a duration of (10.80 ± 0.50) years, and the Hale Cycle has a duration of (21.90 ± 0.66) years (Table 3). Since these solar cycles are well-known (Kuklin 1976), the heightened solar flare activity of 2003 October should not have been surprising. Joselyn et al. (1996) predicted that the maximum of Solar Cycle 23 should occur in early 2000, but with severe geomagnetic storms expected between 1999 and 2005. The unexpected activity detected in 2003 October is in the middle of this latter range, but three years after the expected cycle maximum. This may have happened because the methods currently used to model solar activity typically match amplitudes of successive solar cycles, and do not inherently include models of variability in the length of the cycle.

The analyses of the duration of the sunspot number cycle and the dates of sunspot minima and maxima provided us with independent ways to determine long-term periodicities. Our median trace analysis of the length of the sunspot number cycle provided secular periodicities of 183 - 243 years. This range overlaps with the long-term cycles of ~ 90 - 260 years which were identified

directly from the FFT and PDM analyses of the sunspot number and area data (Figures 3 & 4). The power spectrum analysis of the (O-C) residuals of the dates of minima and maxima provided much clearer evidence of dominant cycles with periods of 188 ± 38 years, 87 ± 13 years, and ~ 40 years.

The derived long-term cycles can be compared with documented epochs of significant declines in sunspot activity, like the Dalton, Maunder, Spörer, Wolf, and Oort Minima (Eddy 1977; Stuiver & Quay 1980; Siscoe 1980). These historic minima correspond to noticeable declines in the average temperatures on Earth. Figure 8 compares the historical sunspot numbers with the derived secular cycles of length (a) 183 years (§4.2), (b) 243-years (§4.2), and (c) 188 years (§4.4). The first two periodicities were derived from the median trace analysis, while the third one was derived from the power spectrum analysis of the sunspot number cycle (O-C) residuals. The fits for the 183-year periodicity all have the same amplitude, but are moderately out of phase with each other, while the fits for the 243-year periodicity are perfectly in phase for all data sets, but with different amplitudes. This figure shows that the 183- and 188-year cycles provide a more consistent match to the sunspot number data than the 243-year cycle, especially during the Wolf, Spörer, Dalton, and Maunder Minima. The modern sunspot number data were combined with early sunspot number data ranging from 1610-1715 (Eddy 1976) and reconstructed (ancient) sunspot number data spanning the past 11,000 years. These reconstructed sunspot numbers are based on dendrochronologically dated radiocarbon concentrations (Solanki et al. 2004). Figure 8 demonstrates that there is a secular periodicity of ~ 188 years in the duration of the sunspot number cycle and that this periodicity is consistent with the geophysical data.

The four historic minima since 1200, all occurred during the rising phase of our derived 188-year sunspot cycle when the length of the sunspot cycle was increasing. Figure 8 shows that, on average, the length of the sunspot cycle was highest when the actual number of sunspots was lowest. According to our model, the length of the sunspot cycle was growing during the Maunder Minimum when there were lower than average reduced temperatures on Earth.

8

TABLE 6
DERIVED LONG TERM SOLAR CYCLES

Data Set	Gleissberg (years)	Secular (years)
Cycle Minima	86.8 ± 8.8	188 ± 40
Cycle Maxima	86.3 ± 18.1	187 ± 37
Combined	86.8 ± 10.7	188 ± 38
Average	86.6 ± 12.5	188 ± 38

The existence of long-term solar cycles with periods of ∼ 200 years is not new to the literature. However, the nature of this cycle is still not understood. Our studies of the length of the sunspot cycle is new and demonstrates that the 188-year cycle is a modulation of the Schwabe Cycle. Jose (1965) noted the coincidence between this long-term sunspot cycle and the 179-year period of the barycentric motion of the Sun about the center of mass of the solar system. Soon & Yaskell (2003) suggested that important barycentric shifts occurred in 1632 (just prior to the Maunder Minimum), 1811 (in the middle of the Dalton Minimum), and 1990. These occurrences seem to be associated with important epochs in the sunspot cycle, however, no physical mechanism has yet been found to link gravitational interactions within the solar system with magnetic activity on the Sun (Soon & Yaskell 2003).

REFERENCES

Bevington, P. R. 1969, Data Reduction and Error Analysis for the Physical Sciences (New York: McGraw-Hill)

Baliunas, S. L., Vaughan, A. H. 1985, Ann. Rev. Astron. Astrophys., 23, 379

Bates, D. M. & Watts, D. G. 1988, Nonlinear Regression Analysis and Its Applications (New York: Wiley)

Coffey, H. E., and Erwin, E. 2004, National Geophysical Data Center, US Department of Commerce & National Oceanic and Atmospheric Administration, Boulder, CO, (ftp://ftp.ngdc.noaa.gov)

Eddy, J. A. 1976, The Maunder Minimum, Science, Vol 192, p. 1189

Eddy, J. A. 1977, The Solar Output and Its Variation, ed. O.R. White, p. 51 (Boulder: Colorado Associated University Press)

Hathaway, D. H. 2004, Royal Greenwich Observatory/USAF/noaa, Sunspot Record 1874-2004, (http://science.nasa.gov/ssl/pad/solar/greenwch.htm) NASA/Marshall Space Flight Center, Huntsville, AL

Hoaglin, D., Mosteller, F., and Tukey, J. 1983, Understanding Robust and Exploratory Data Analysis (New York: Wiley)

Jose, P. D. 1965, A.J., 70, 193

Joselyn, J. A., Anderson, J., Coffey, H., Harvey, K., Hathaway, D., Heckman, G., Hildner, E., Mende, W., Schatten, K., Thompson, R., Thomson, A. W. P., and White, O. R. 1996, Solar Cycle 23 Project: Summary of Panel Findings (http://www.sec.noaa.gov/info/Cycle23.html)

Kuklin, G. V. 1976, Basic Mechanisms of Solar Activity, IAU Symp. No. 71, ed. V. Bumba, J. Kleczek, p. 47 (Boston: Reidel)

Lupton, R., & Monger, P. 1977, The SuperMongo Reference Manual

Press, W. H., Teukolsky, S. A., Vetterling, W. T., & Flannery, B. P. 1992, *Numerical Recipes in FORTRAN: The Art of Scientific Computing* (Cambridge: Cambridge University Press), 2nd edition.

Richards, M. T., Waltman, E. B., Ghigo, F., & Richards, D. St. P. 2003, ApJS, 147, 337

Siscoe, G. L. 1980, Rev. Geophys. Space Physics, 18, 647

Solanki, S. K., Usoskin, I.G., Kromer, B., Schüssler, M., & Beer, J. 2004, Unusual Activity of the Sun During Recent Decades Compared to the Previous 11,000 Years, Nature, Vol. 431, No. 7012, p.1084

Soon, W., & Yaskell, S. H. 2003, The Year Without A Summer, Mercury, Vol. 32, No.3, p. 13

Stellingwerf, R. F. 1978, AJ, 224, 953

Stuiver, M., & Quay, P. D. 1980, Science, 207, 11

Topping, J. 1972, Errors of Observation and Their Treatment (London: Chapman & Hall)

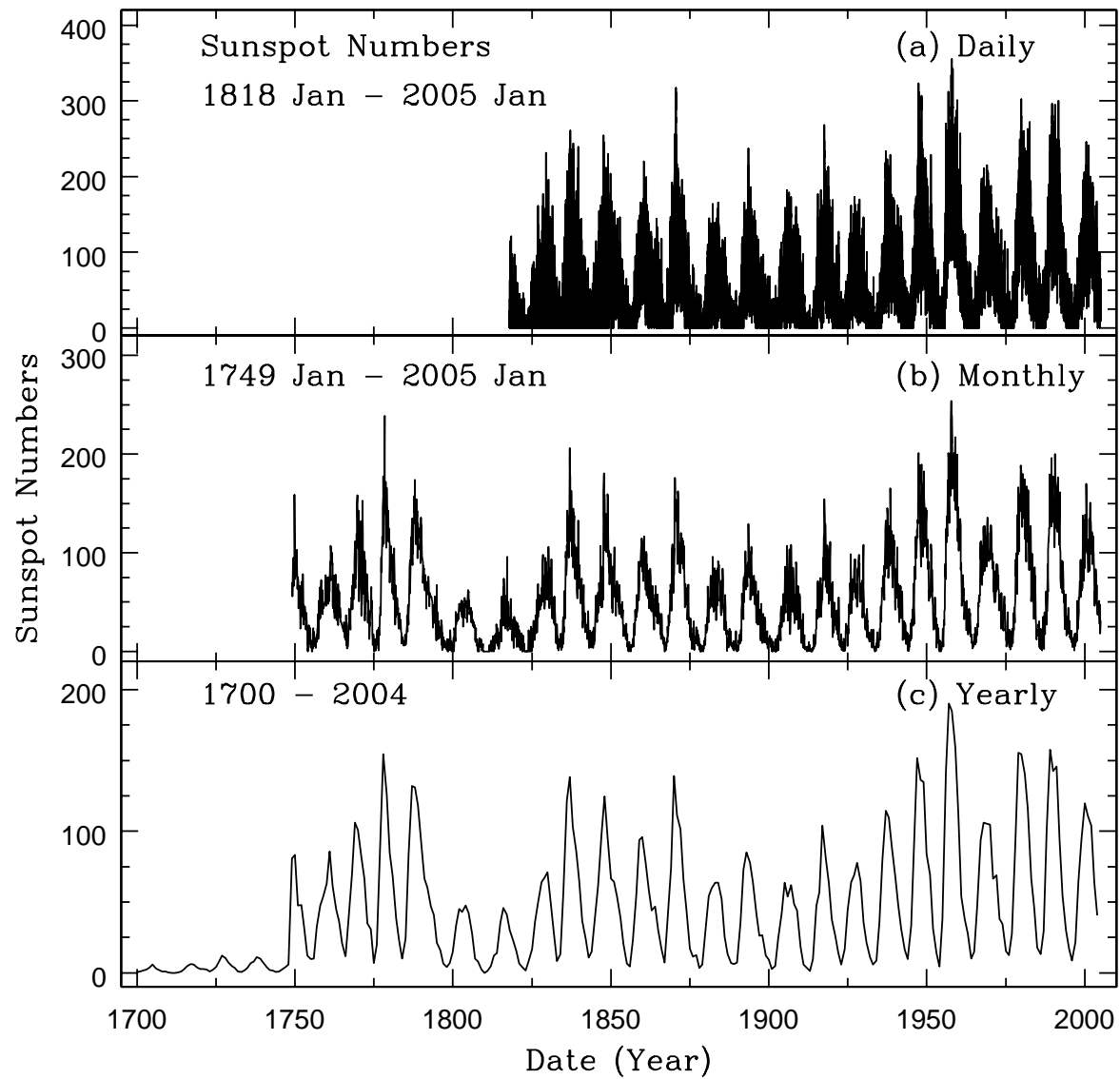Wilson, P. R. 1994, Solar and Stellar Activity Cycles (New York: Cambridge University Press)

Fig. 1.— Archival data for (a) daily, (b) monthly, and (c) yearly sunspot numbers from 1700 to 2005.
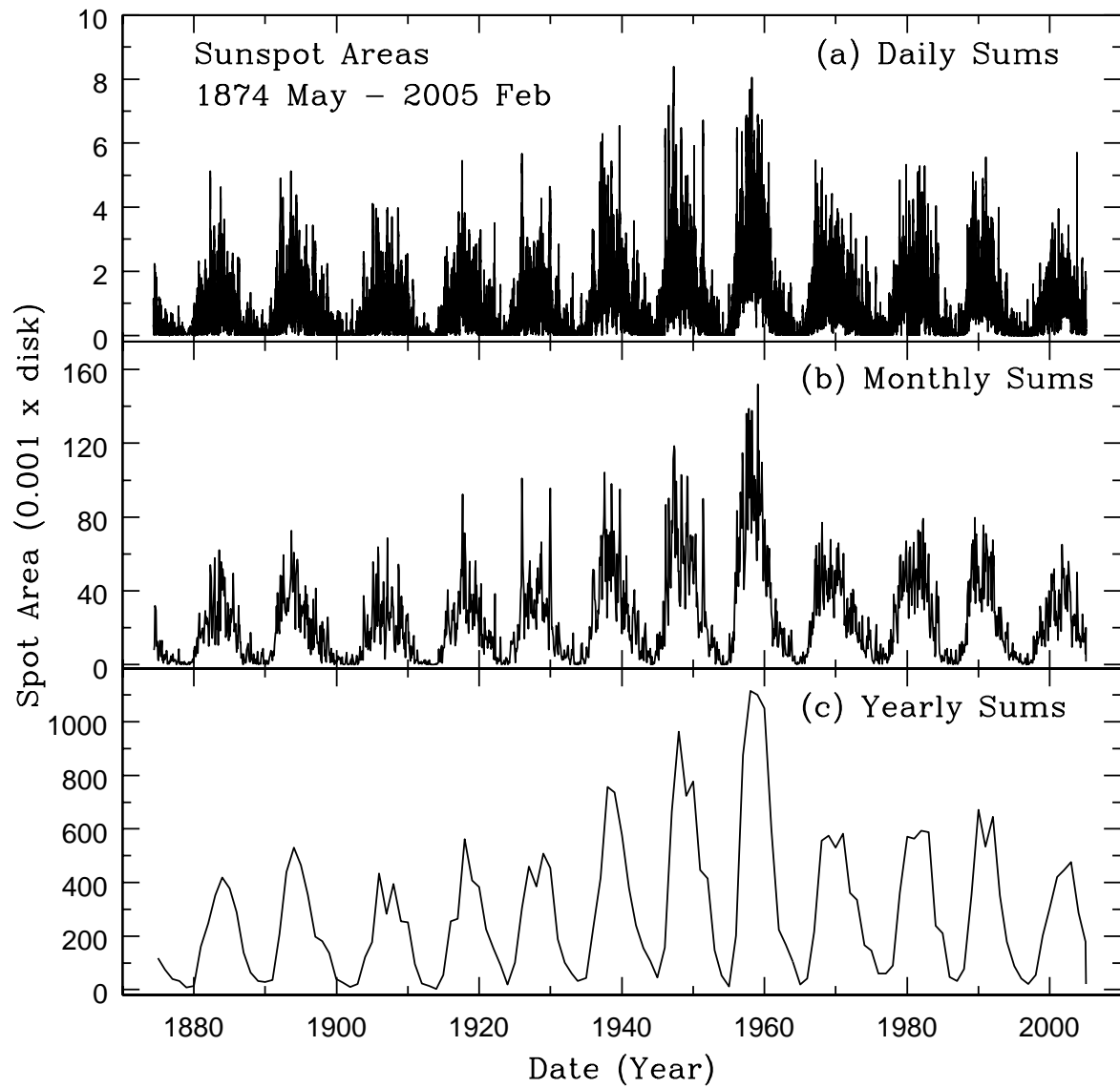
11

Fig. 2.— Archival data for (a) daily, (b) monthly, and (c) yearly sums of whole sunspot areas (0.001 x Solar Hemispheres) from 1874 May to 2005 February.
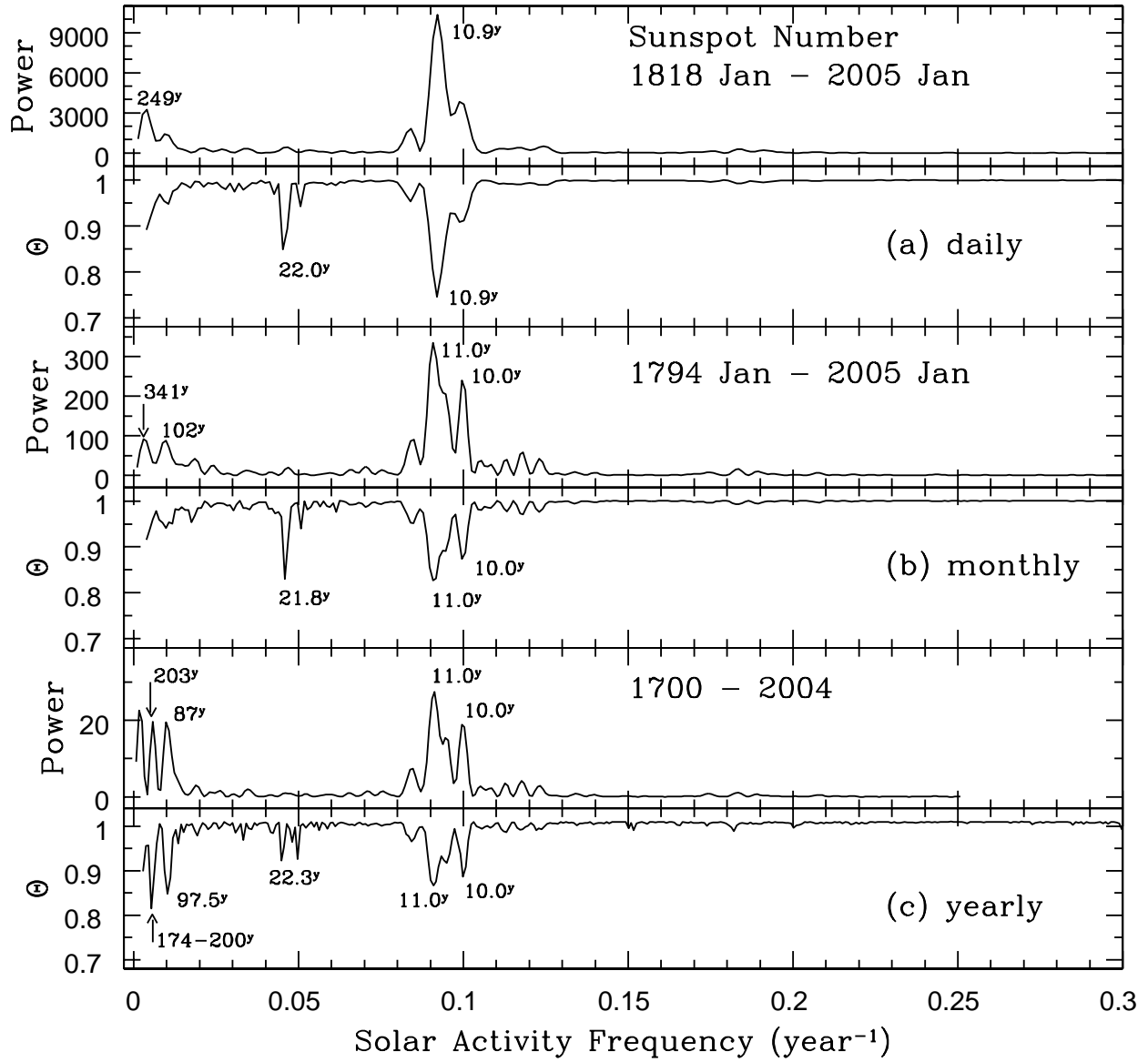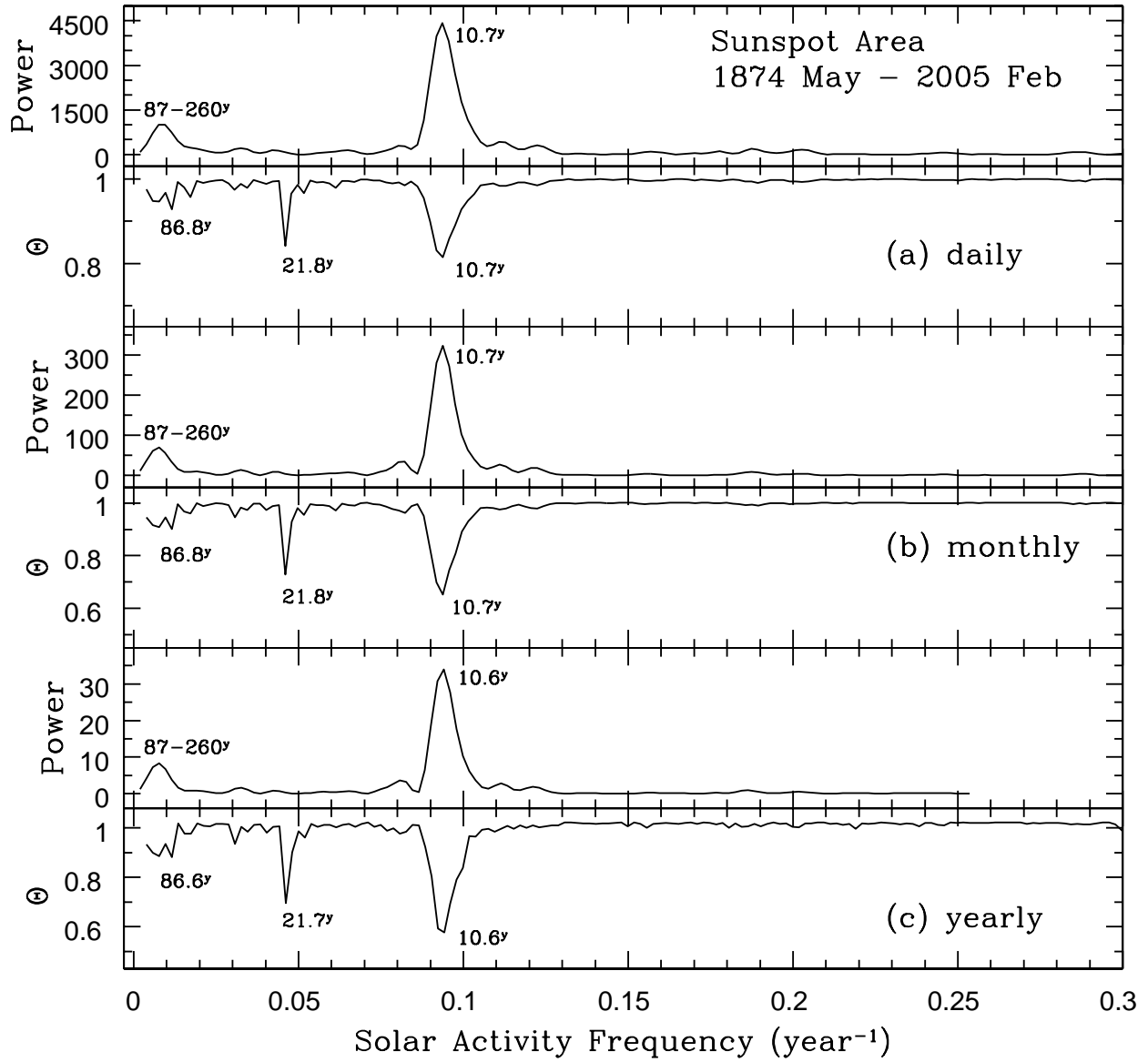
Fig. 3.— Frequencies of solar activity derived from power spectrum (upper frame) and PDM (lower frame) analyses calculated from (a) daily, (b) monthly, and (c) yearly sunspot numbers. The labels within the plot show the durations of the derived cycles in units of years.

13

Fig. 4.— Frequencies of solar activity derived from power spectrum (upper frame) and PDM (lower frame) analyses calculated from (a) daily, (b) monthly, and (c) yearly sums of sunspot areas from 1874 May to 2005 February. The labels within the plot show the durations of the derived cycles in units of years.

14
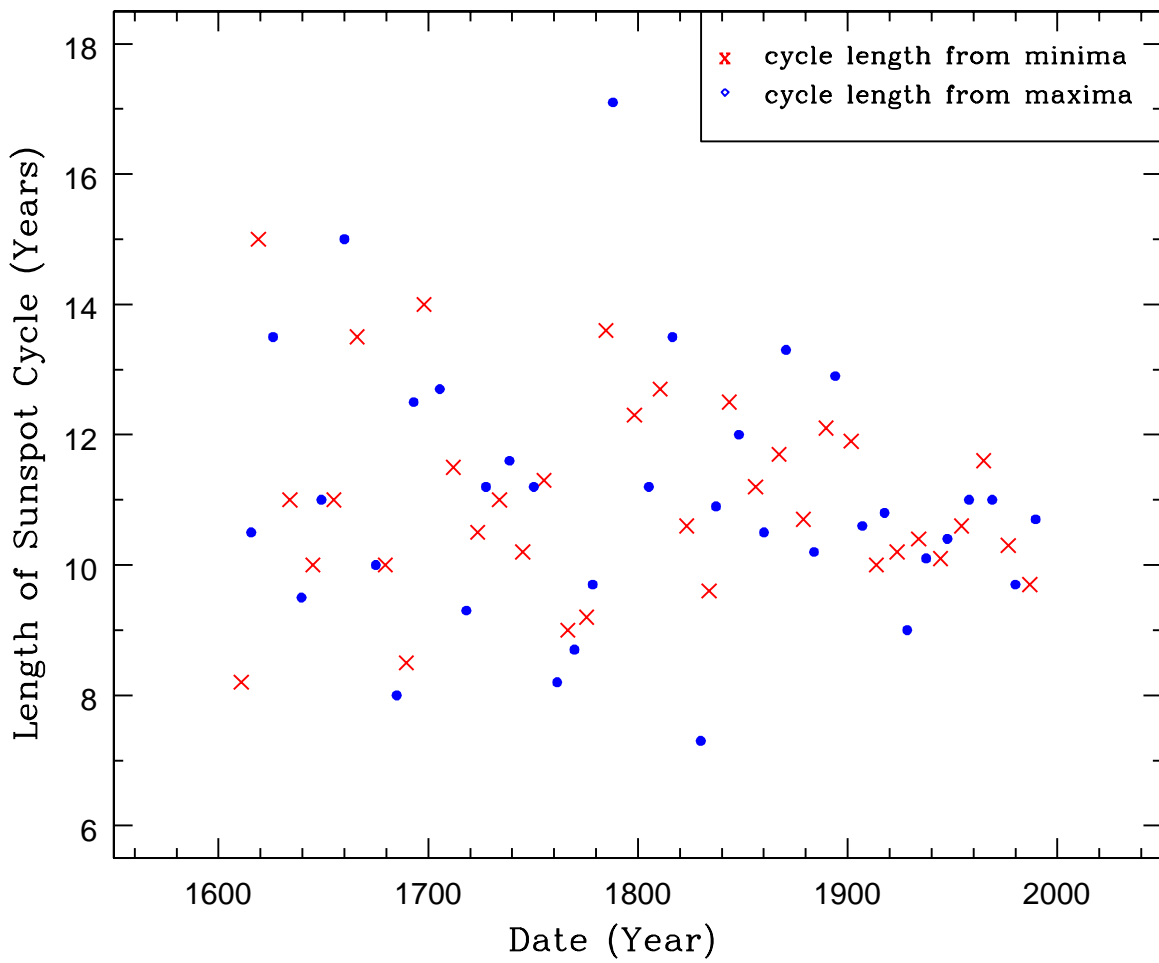
Fig. 5.— Sunspot cycle durations derived from successive minima (red crosses) and successive maxima (blue dots) for dates from 1610.8 to 1989.6.
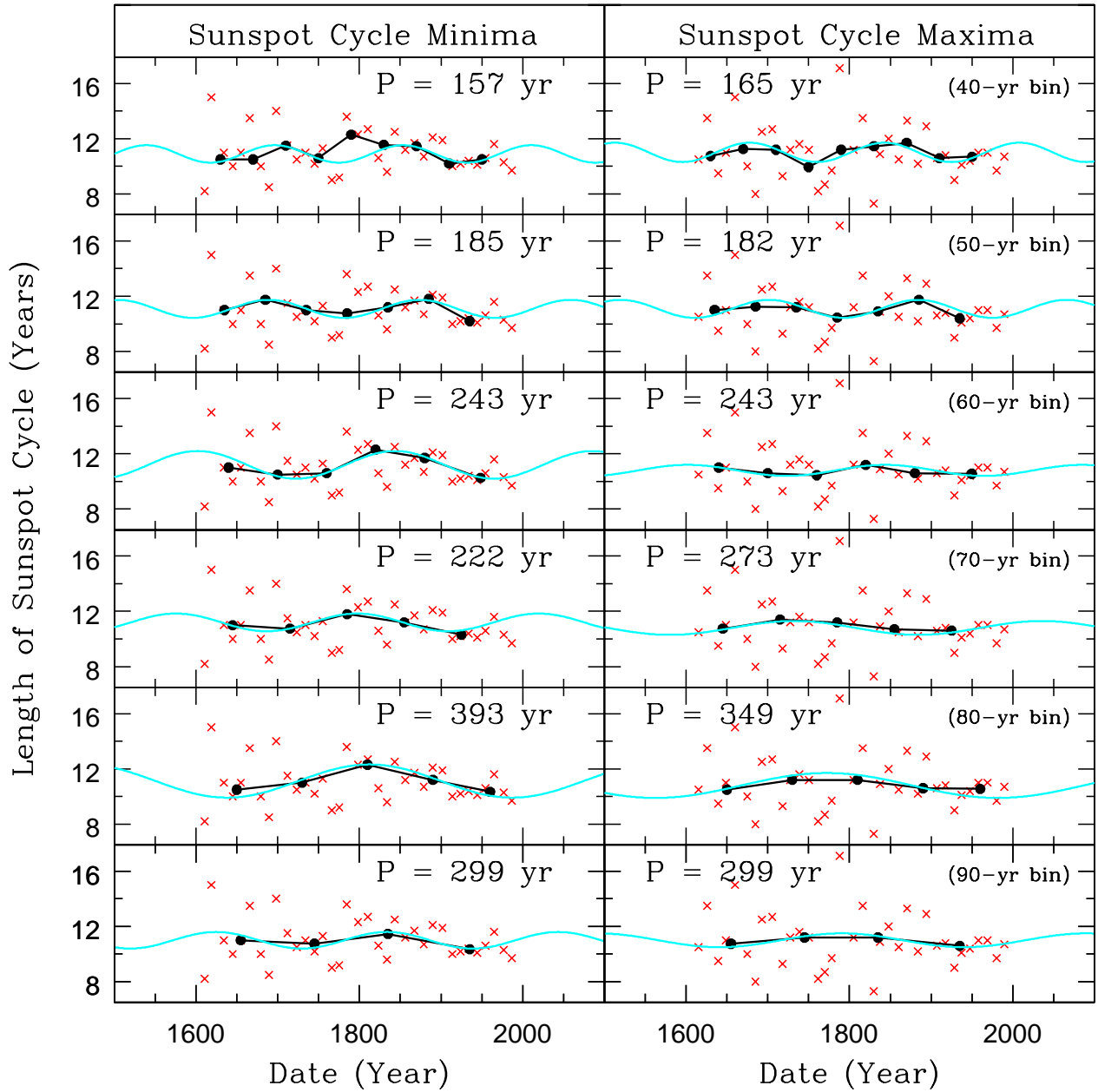
Fig. 6.— Median traces for sunspot minima and maxima derived with bin widths of 40 - 90 years. A sinusoidal fit to the median trace is shown for each bin width. The average period of each derived sinusoidal fit is given at the top of each frame.
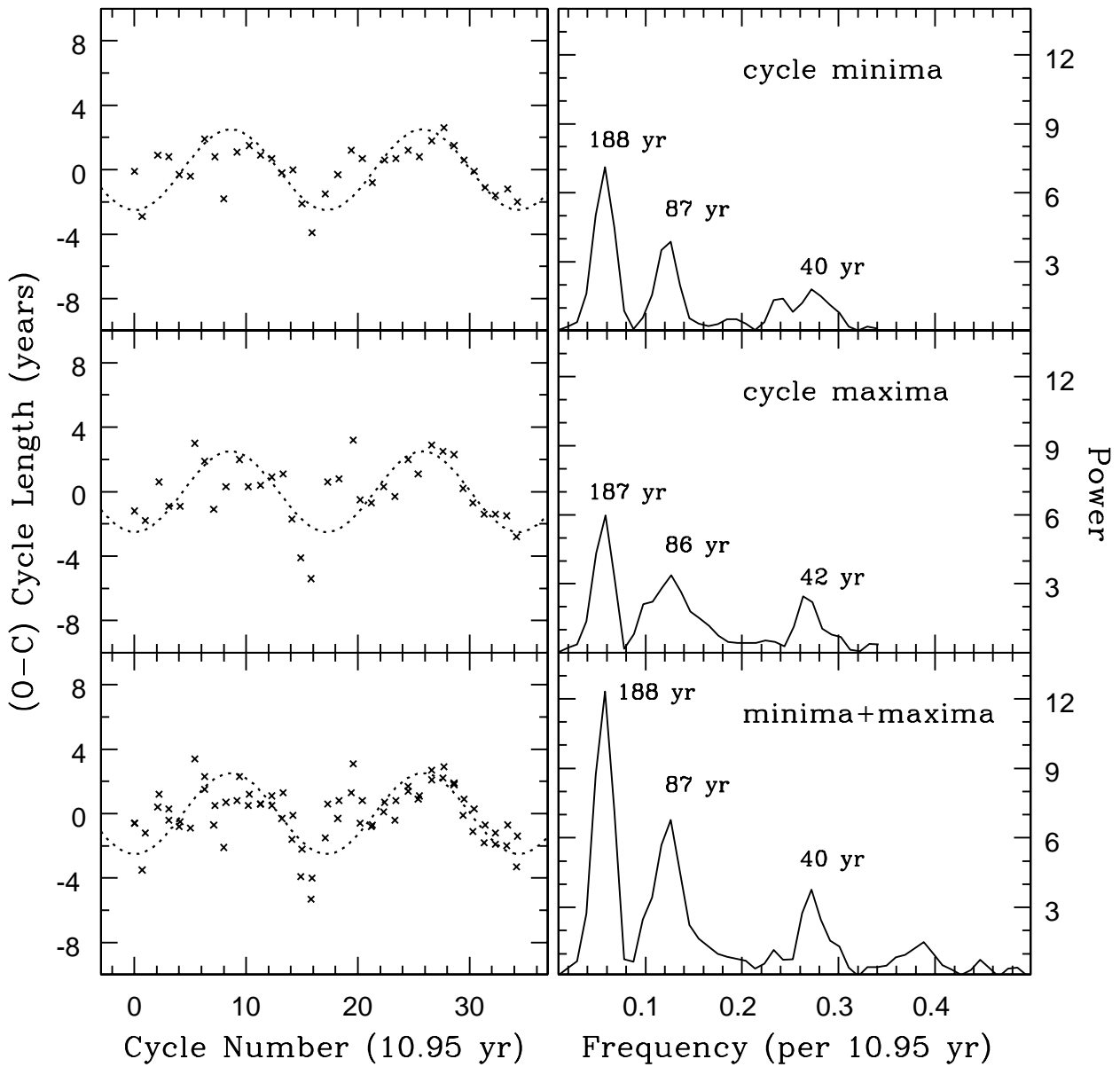
Fig. 7.— The cycle length (O-C) residuals (left frames) and the corresponding power spectrum (right frames) for the sunspot cycle minima (top frame), maxima (middle frame), and combined minima and maxima data (bottom frame). The dashed line through the data represents the long term cycle derived from the power spectrum analysis.
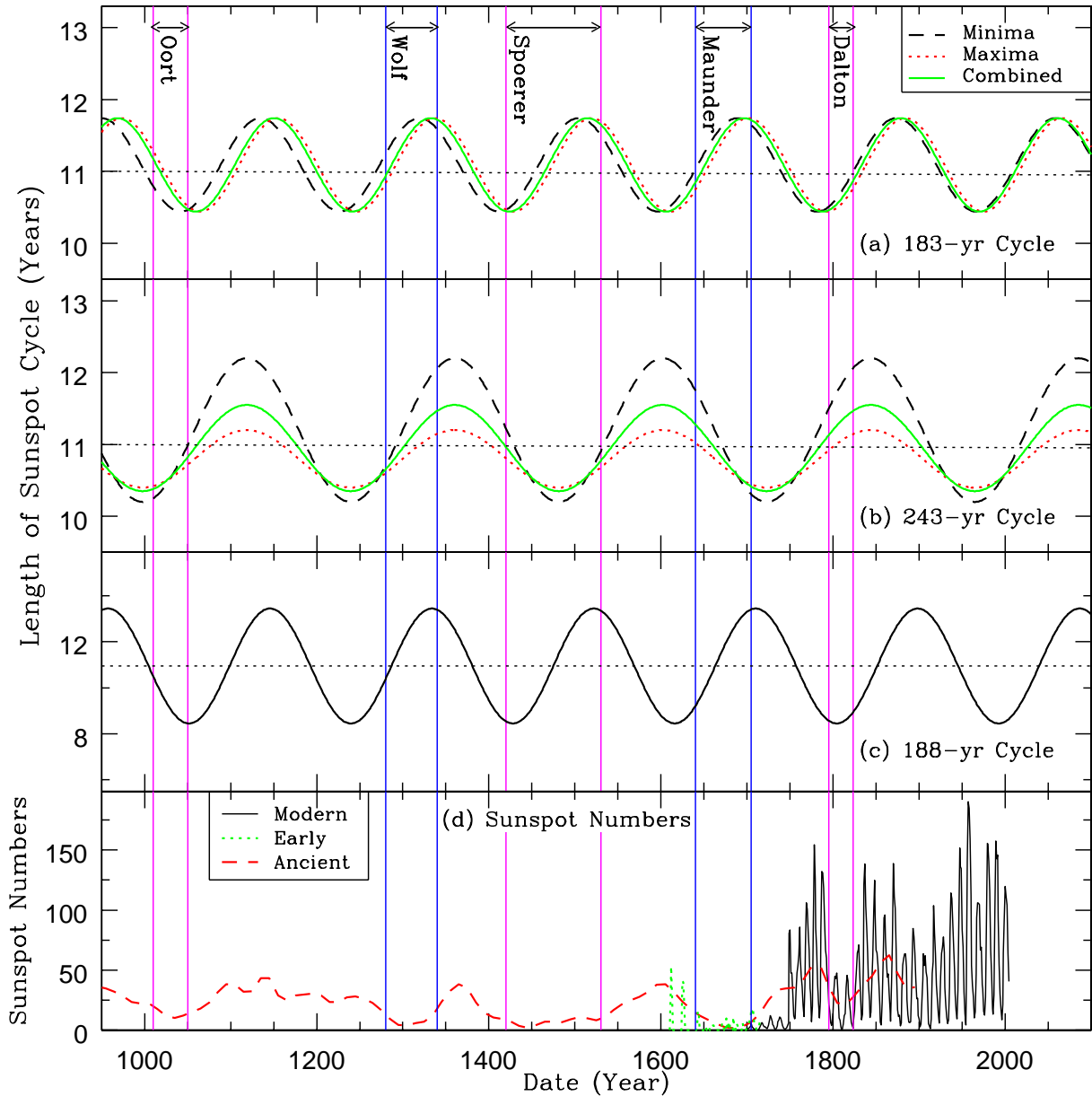
Fig. 8.— Sinusoidal fits to the sunspot number cycle corresponding to the derived periods of (a) 183 years, (b) 243 years, and (c) 188 years, compared with (d) the sunspot number data. The fits to (a) and (b) were produced from binned cycle minima (dashed line), cycle maxima (dotted line), and a combination of the two data sets (solid line). The bottom frame shows sunspot numbers from 1700-2004 (modern, solid line), 1610-1715 (early, dotted line), and 950 - 1950 (ancient, dashed line) reconstructed from geophysical data. The Dalton, Maunder, Spörer, Wolf, and Oort Minima are identified on the graph. The dates of these historical minima correspond well with the derived periodicities of 183 and 188 years, except for the Oort Minimum. The 243-year cycle does not match the historical minima as well as the other periodicities.